Borehole thermal energy storage (BTES). First results from the injection phase of a living lab in Torino (NW Italy)

Published version:

DOI:10.1016/j.renene.2015.08.052

Please cite this Manuscript as Giordano N., Comina C., Mandrone G., Cagni A. (2016) – Borehole thermal energy storage (BTES). First results from the injection phase of a living lab built up in unsaturated alluvial deposits (Torino, IT). Renewable Energy, 86: 993-1008.

UNIVERSITÀ DEGLI STUDI DI TORINO

This is an author version of the contribution published on:

[Renewable Energy, 86, 2016, 10.1016/j.renene.2015.08.052]

The definitive version is available at:

[https://www.journals.elsevier.com/renewable-energy/]

Borehole thermal energy storage (BTES). First results from the injection phase of a living lab in Torino (NW Italy).

N. Giordano[1], C. Comina[1-2], G. Mandrone[1-2], A. Cagni[3]

[1] Earth Science Department – Torino University, Via Valperga Caluso, 35 – 10125 Torino (IT)
[2] AG3 srl – A Spin Off Company of Torino University, Via Valperga Caluso, 35 – 10125 Torino (IT)
[3] EQ Ingegneria – Ghibaudo Cagni Zilioli Associati, Strada Dronero, 13/A – 12022 Busca (CN, IT)

Corresponding Author
Nicolò Giordano
Via Valperga Caluso, 35 – 10125 Torino (IT)
nicolo.giordano@unito.it
tel: +39 011-6705325
fax: +39 011-6705128

Abstract

The seasonal storage of thermal energy in the ground is a useful application able to provide H&C and DHW demand of commercial or residential buildings. Several examples in Canada and Northern Europe demonstrated the reliability and convenience of these systems in terms of both energy and economic savings, but more demonstration sites are however necessary. The surrounding litho-, hydro- and bio-sphere are influenced by the plant's activity and a trustworthy supervision of the temperature field would bring advantages to both the environment and the system's efficiency. Usually numerical modeling is used to forecast the system behavior but results of simulations can be strongly dependent from assumed material characteristics and should be strictly calibrated on real data. To better understand thermal processes in the ground related to thermal injection and thermal storage, a field scale BTES living lab was build up nearby Torino (Northern Italy) within unsaturated alluvial deposits. Results show that approximately 9.1 GJ were transferred to the ground during the first year, raising the undisturbed temperature by 2°C, and that a correct comparison of monitoring data and numerical simulations can be obtained following a specific site characterization.

Keywords: borehole thermal energy storage; sensible heat; numerical simulation; porous media; Italy

1. INTRODUCTION

The idea of exploiting the energy provided by renewable sources has been always accompanied by the problem that most of these sources can supply energy when the user's demand is low. The thermal energy storage (TES) is a highly debated concept which was first mentioned in the late 1970s. In recent years several storage technologies have been developed in order to find some valid solutions which can assure criteria of reliability, efficiency and economic sustainability.

One of these solutions consists in generating the heat from the Sun and accumulating it in the ground in order to face the day/night and summer/winter alternation in the solar productivity. The system uses the ground as a medium for daily (short term - ST) or seasonally (long term - LT) storing of the heat through borehole heat exchangers (BHEs) which connect the heating source and the storage volume. Hence, the ground thermal energy storage falls back in the category of the low enthalpy geothermal systems, which typically exploit the ground as a source using BHEs coupled with heat pumps to cover the thermal energy demand of the buildings. In both cases the ground has an active part in generating thermal energy, but in thermal storage applications it plays a double role: on one side it should accumulate as much heat as possible (storage medium), minimizing the losses through the surrounding subsurface and the atmosphere; on the other it has to provide the stored heat as long as necessary (source).

The interaction of such systems with the ground is doubtless non-trivial. Nevertheless, the underground part of the plants is too often modestly debated, minimizing the problem to the number and depth of the BHEs, taking under consideration an average linear productivity value, if specific thermal response tests cannot be carried out. It is conversely necessary to test this part of the plant from multiple points of view in order to construct a system sustainable and perfectly integrated in the litho-, hydro- and bio-sphere. A correct sizing of the plant will benefit not only its efficiency but also the health of the environment.

Hence, the present study arises from the necessity to better understand the ground's behavior when affected by thermal injection, both for the efficiency of the energetic system and for subsurface monitoring. This paper presents the natural consequence of a wider research activity firstly applied at laboratory scale consisting in: i) analogical/numerical modeling of thermal injections in porous media, in order to test the ability to transfer and store the heat as a function of the water content **[1]** and ii) electrical resistivity measurements tested as a monitoring tool for the imaging of the heated plume's distribution **[2]**. In the light of the laboratory's outcomes, a small scale BTES plant was built up near Torino as a monitoring and field scale laboratory site to evaluate the ground's ability to conduct and store the thermal energy. The plant was officially launched on 2014, April 2 and the results of the first operative year are here presented together with numerical simulation outcomes. The geophysical methodology applied for the monitoring activity will be discussed in a second paper.

2. STATE OF THE ART ON BOREHOLE THERMAL ENERGY STORAGE

The Sun provides an enormous amount of energy, about 3.8 x 10^{18} J (i.e. 1 x 10^{12} kWh y^{-1}). Nevertheless, this abundant amount of energy has an intermittent character owing to the day/night alternation and the passing of seasons. This time-dependent supply does not match with the human needs and the misalignment between the source and the demand is one of the longstanding barriers to solar energy technology. The peak demand occurs in the late evening when the solar radiation is no longer available, while the peak supply takes place in the middle of the day when generally both electricity and thermal energy demands are at the daily minimum. The wide solar technology spreading in the last 5 years in Italy and the installation of several small-medium size photovoltaic plants for power production have modified the daily supply curve, lowering the price of the electrical energy at the Stock Exchange at a minimum in the middle of the day. In particular, on 2013 April 14 the electricity price collapsed to almost 0 € MWh^{-1} at 3 PM and rose to about 90 € MWh^{-1} just 6 hours later **[4]**. There is therefore a significant amount of low cost energy available that can be exploited.

The solar energy can therefore potentially lead the energetic transition from fossil fuels to renewable sources but storage mechanisms have to be implemented in order to bridge the gap between the energy source and its application to buildings and facilities. The development of several storage technologies able to reduce the time and rate of the supply/demand mismatch and the strong commitment of the leading countries in the efficiency are driving the energy revolution of the present decades, aiming at the increasing sustainability of the human activities.

Two key factors in selecting the material for the energy storage are the energy density, defined as the amount of energy accumulated per unit volume or mass, and the operation temperature range (**[5]**). The amount of thermal energy E [J] stored in a volume of material can be expressed as:

$$E = \gamma_b \cdot Cs_b \cdot V \cdot \Delta T \qquad [1]$$

where γ_b [kg m^{-3}] and Cs_b [J kg^{-1} K^{-1}] are the bulk density and the specific heat capacity of the storage medium, V [m^3] is the volume and ΔT [°C] is the temperature range of operation.

According to Pilkington Solar International GmbH **[7]**, any TES system can be classified by storage concept and by storage mechanism. Based on the former, the systems can be active if they are characterized by forced convection and the storage medium itself circulates alone (direct or closed loop systems) or different media are used to collect and store the heat (indirect or open loop systems). Conversely, they can be passive if a heat transport medium passes through the storage medium to charge or discharge it by thermal energy. The storage medium can be a liquid, a solid, a phase change material or a chemical reactant. The storage mechanisms, together with the storage materials involved, have been researched intensively in the frame of Task 32 **[8]** and Task 42 **[9]** of the IEA Solar Heating and Cooling (SHC) programme. Three main categories can be identified on the strength of the storage mechanisms: chemical heat, latent heat and sensible heat, the formers being the ultimate innovative technologies while the latter deriving from decades of research and experiments. Details on chemical storage and adopted thermo-chemical materials (TCMs) can be found in Errore. L'origine riferimento non è stata trovata.**[10]**, **[11]**. In-depth analysis on techniques and phase change materials (PCMs) involved in latent heat storage applications can be conversely found in **[14]**, **[15]**, and **[16]**.

The sensible heat, which is among the storage mechanisms the most popular and most practiced in the last decades, is the internal energy of a substance which undergoes a temperature increase without changing its phase. Sensible heat storage technologies are easy to control and mostly environmental friendly, with material costs far lower than latent and chemical applications. Conversely, they need to involve large volumes owing to the low energy density. The huge volumes required on turn influence the self-discharge problems and the high initial investment due to the construction activities. **Fig. 1** highlights the differences among the three mentioned storing methodologies by showing volumes needed to store 10 GJ of energy with a temperature range of operation equal to 70°C as proposed by **[17]** in a report of the IEA SHC Task 32. Comparing the volumes necessary when a porous medium fully (quaternary sediments below the groundwater table) or half saturated (quaternary sediments in the vadose zone) by water or a compact granite is used as storage material it is evident that it would need a volume of rock or unsaturated deposits 2 times bigger than a volume of water in order to accumulate the same amount of energy. But a saturated porous medium with an average porosity of 0.35 would require only 25% more volume than what the water needs. Nevertheless, there is no comparison between sensible heat storage materials and those involving latent (PCMs) and chemical (TCMs) heat. Apart from the quantity of material, its dimensions are also important, being fundamental a low surface/volume ratio for minimizing the heat losses **[5]**.

Besides density and specific heat of the storage material (energy density), other properties are important for sensible heat storage: the thermal conductivity and diffusivity, the temperature range of operation, the stratification of the storage unit and the heat loss coefficient as a function of the surface areas to volume ratio. Details on stratification concept can be found in **[18]**, **[19]**, **[20]**, **[21]**, **[22]**, **[23]**, **[24]**, and **[25]**. The most popular material for applying the sensible heat storage is the water, which has noticeable heat capacity (4.2 x 10^6 J m^{-3} K^{-1}) and it is easy to manage by pumping it. Water is often used alone in artificial tanks (**[24]**, **[26], [27]**, **[29]**, **[30]**) or from aquifers in open loop systems (**[30]**, **[32]**), solar ponds (**[33]**, **[25]**) and underground caverns and holes (**[35]**) sometimes previously used for oil storage. A high thermal conductivity can promote injection and extraction of heat, but at the same time it can cause system's self-discharge. Rocks and geological porous media are used as storage material as well, because of their widespread availability and their low heat loss rate compared to water. Rocks have good thermal capacity (2-3 x 10^6 J m^{-3} K^{-1}) and conductivity (3-5 W m^{-1} K^{-1}), but they often present a high fracturing state which can lead to self-discharge caused by water flows. The quaternary deposits show rather high heat capacity if saturated by water, but groundwater flow could carry away the heat. Rock bed storage systems consist of volumes of pebbles, gravels or concrete bricks completely saturated by a heat transport fluid (air or water) which circulates through it charging and discharging thermal energy (**[15]**, **[19]**, **[30]**, **[36]**).

Nevertheless, this key factor is related not only to intrinsic characteristics of the material, but also to the environmental conditions of the site. Geological materials are therefore freely available, but several geological conditions need to be analyzed beforehand for their fruitful use (**[38]**). Geological requirements need to be accounted for in the early stages of the project in order to select the system that can provide the best efficiency and the lowest environmental impact. Research studies in this field have to aim at the optimization of storage temperatures, insulation technologies and material properties. In addition, a real scale simulation and a numerical model calibrated on experimental direct or indirect data are essential to understand the ground's behavior and to highlight the affecting factors. Definitely, all these consideration have to be taken into account when choosing the type of system according to available space, geological and hydrogeological conditions, difficulties in the local authority approval procedures and final user's requirements.

From an operational point of view, the plant generally consists of a thermal collectors' area (usually on the roofs of the supplied buildings), a ST storage called "buffer storage" (very often simple water tanks), a LT storage and a heat distribution network **[30]**. The purpose of the buffer storage (when present) is to minimize the transients in the energy delivery due to day/night alternation and bad weather days, which can affect energy collection **[7]**. It is very important to transfer heat to the LT storage at a constant temperature throughout the warm season, or at least to have the opportunity to choose which part of the volume to supply.

The underground can be profitably used for storing the thermal energy in a closed-loop system, involving borehole heat exchangers in vertical (**Fig. 2**) or horizontal disposition (**Fig. 3**). In the first type a series of BHEs is drilled in the ground (typically in number of 30-50) down to 40-50 m, which is lower than the classical depth of ground coupled heat pumps (GCHPs). The ratio surface to volume should be always as much low as possible in order to minimize the losses towards the surrounding ground. A layer of insulation materials is predisposed on top of the boreholes. The insulation is also applied above the set of pipes linking the storage volume to the buffer storage of the system, because the largest losses occur towards the atmosphere. Sometimes the volume is also insulated at the side walls, but the costs are definitely not negligible. Among all the described applications, the closed-loop ground-based storage systems have the lowest energy density with around 15-30 kWh per cubic meter of ground. The water-based storages possess a 60-80 kWh m^{-3} energy density, while the gravel-water mixtures and the aquifer systems attest to approximately 30-50 kWh m^{-3} **[40]**.

A common borehole disposition consists of a circular shape with a radius in the range 15-30 m (on the strength of the needed volume) and a spacing of less than 1 m among the heat exchangers. This arrangement permits creating a warmer core in the center of the cylinder and an annular zone around it becoming colder and colder towards the exterior. The hydraulic circuit usually operates in order to transfer the heat first in the central pipes and then in cascade in the external **[41]**. Indeed, the boreholes are hydraulically connected in series or in parallel. During the charge of thermal energy, the flow direction is from the centre to the boundaries in order to achieve high temperature in the core and lower values in the externals. In the cold season flow direction is reversed and heat is first extracted from the boundaries progressing towards the core **[30]**. This working mode allows achieving several targets: (i) the core is always supplied with the warmer thermo-vector fluid and is heated up continuously; (ii) the fluid going out from the central BHEs is still carrying a not negligible amount of heat and this is used for heating up the lateral portions; (iii) the gradient between the core and the undisturbed ground is lowered by the temperature in the annular zone, promoting a low self-discharge of the system; (iv) a modular design allows adding supplementary boreholes afterwards, which can be easily connected for the growth of the system.

In the following tables, several plants with BTES technology are reported with detailed features for each system. Sweden (**Tab. 1**) and Germany are the countries with the highest experience since the 1980s until the current time, but other nations have contributed to the knowledge as well (**Tab. 2** and **Tab. 3**).

3. MATERIALS AND METHODS

3.1 Geographical, climatic and geological context

The test site is situated near Torino in the municipality of Grugliasco (geographical coordinates 45° 3' 55'' N, 7° 35' 23'' E). It is located in the north-western portion of the *Pianura Padana*, between the Sangone River on the South, the Po River on the East and the Dora Riparia River on the North. The elevation of the area is 287 m a.s.l., with a difference of approximately 70 m with respect to the Po River level. The site receives a solar radiation which allows producing approximately 1,300 kWh m^{-2} per year and is characterized by 2,092 heating degree-days referred to 18°C (**Tab. 4**).

The first operative year of the system built up in Grugliasco was characterized by a summer period different from what usually expected in North-Western Italy. This can be noted from a comparison of the average daily temperature and the monthly rainfalls between the periods April - October 2014 and April - October 2005 – 2013 (**Fig. 4**). The 2014 data were registered by a weather station placed in the *Physics Department* **[50]**; the 2005 - 2013 data belong to *Arpa Piemonte* **[51]**. The weather station is located in the Torino city being aware that the air temperature in Grugliasco would be approximately 2°C smaller. Since May to September 2014 the temperature was clearly smaller than the average; in particular, July and August registered values around 21°C, being the average standing approximately at 24°C. In addition, July 2014 was the rainiest among the last ten years together with July 2011. June and September were the second and the first driest months among the considered period while August stood around the average.

From the geologic point of view the area consists of abundant Pleistocene-Holocene glacio-fluvial coalescing fans connected to the alluvial plain of the Po River, which on turn lays on the Torino Hill lithological units (**Fig. 5**). The plain consists of gravelly-sandy materials with high permeability in the first 60-70 m below the ground level (**Fig. 6**). Within these deposits it is common to find layers of compacted gravels or conglomerate (the "Ceppo"), deriving from the cementation of gravels by a carbonatic cement of fluvio-glacial origin. In the test site the surficial deposits belong to "*Subsintema di Col Giansesco*" (Pleistocene Inf. - Holocene) which is part of the "*Sintema di Frassinere*": in this unit pebbles of quartzite, serpentinite, gneiss, prasinite and calcareous schist were found **[52]**. Below this unit, there are deposits of a transitional *facies* between marine and continental environment, being characterized by the alternation of coarse sands and silts due to the progression and regression of the coastal line in the Pliocene Med. – Pleistocene Inf.

Drilling activity performed in the site confirmed the overall geological setting and showed 30 m of gravels and sands. Sometimes some decimetric layers of compacted gravelly sands were encountered. Samples, pertaining to these levels, collected for laboratory analyses, revealed the presence of carbonatic cement in the matrix. Other samples of un-compacted gravels and sands (sampled at 7.5, 21 and 27 m depths) were moreover analyzed for the determination of the grain size distributions (**Fig. 7**). These samples were also analyzed from a thermal point of view (**Tab. 5**), whereas it was not possible to examine the compacted samples because of the presence of too big pebbles. The devices adopted for thermal characterization were the ISOMET 2114 (*Applied Precision Ltd., Bratislava*, SK) and the KD2 Pro (*Decagon Devices Inc.*, Pullman, WA, USA), which can measure properties of both porous media and rocks. The ISOMET 2114 (ISO) is based on the transient line source method and it applies the dynamic measurement method in order to minimize the measurement time. For the determination of the thermal conductivity of the examined samples the needle probe IPN 1100 was used (measurement range 0.015 – 2.0 W m^{-1} K^{-1}, accuracy 5%). The KD2 Pro device (K2D), based again on the transient line heat source method, applies different algorithms on the strength of the selected probe (dual needle or single needle). The conductivity was measured with the TR-1 single-needle probe (measurement range 0.1 - 4.0 W m^{-1} K^{-1}, accuracy 10%). Contrary to the ISO, this probe has a larger diameter and provide longer heating time for minimizing the errors related to the contact resistance. In addition, TR-1 heats the sample significantly more than IPN 1100 on the ISO, making possible to measure higher λ values.

From the hydrogeological point of view, a phreatic aquifer is hosted in the shallower unit, while the deeper unit is characterized by a multi-level aquifer. The groundwater in the first unit flows eastward, being in direct connection with the Po River. On the strength of the available data, the water table in the examined area is thought to stand to 35-40 m below the ground level. On the basis of the grain size distributions of the 3 collected samples, the hydraulic conductivity K [m s^{-1}] was calculated with the Kozeny-Carman equation **[53]**. Values of $K = 2.3 \times 10^{-4}$, 5.6×10^{-4} and 3.5×10^{-4} m s^{-1} were respectively obtained.

3.2 Plant's setup

In the light of the above described geological conditions and owing to administrative regulations, the plant was set up in the unsaturated zone of the unconfined aquifer. This situation was however a valuable choice in order to test the ability of unsaturated saturated alluvial deposits in storing the heat. Following the evidences of laboratory simulations on similar materials **[1]** intermediate (25 - 50 %) water content showed indeed great potentiality in storing the heat. The underground part of the system was located nearby the Topography building of the *Department of Agricultural, Forest and Food Sciences of Torino University* (**Fig. 8**). It stores the heat in the ground by means four 27 m deep BHEs. The arrangement consists of a double-U piped borehole placed in the center of an equilateral triangle (2 m side), and other 3 single-U piped BHEs located at the triangle's vertexes (**Fig. 9**). A 33 m deep monitoring hole was moreover located 2 m away from the double-U heat exchanger. The top of the BHEs is placed at a depth of 1.5 m from the ground level in order to minimize the heat losses towards the atmosphere. The distance between the BHEs and the building is more than 10 m and it was therefore important to cover all the connecting pipes with a 1.5 m thick insulating layer for preventing the heat losses.

The grout used for guaranteeing a valuable thermal connection between the pipes and the surrounding ground has a nominal thermal conductivity of $\lambda = 2$ W m^{-1} K^{-1}. Two days after the end of the drilling activity, 3 samples of the grout were collected and analyzed with both the ISO and the KD2 (**Tab. 6**). With the first device, the surface probe IPS 1100 was used (measurement range 0.04 – 6.0 W m^{-1} K^{-1}, accuracy 10%), while with the second the TR-1 was adopted. In this case the most reliable values should be those measured with the ISO because for compacted and previously smoothed samples the surface probe seemed more appropriate. Measured grout thermal conductivities where notably lower than the nominal one (**Tab. 6**) and could potentially affect the system behavior for these kind of applications. Nevertheless in the unsaturated deposits at the test site the effective λ of the ground is rather low (see **Tab. 5**) and thus comparable to the grout. The material surrounding the pipes can be therefore considered thermally homogeneous.

The remaining part of the system was located in the Topography building. Two solar thermal panels were placed on the roof with a total net surface of 5.0 m^2 with an inclination of approximately 10° (**Fig. 9**). Typically, the solar collectors are installed with an inclination of 30° for guaranteeing a valuable production also in winter, when the Sun's orbit is low and the delivery daily hours no more than 3-4. Nevertheless, in this case a low inclination arrangement was provided in order to maximize the production in the summer period and in the central part of the day (see **Tab. 4**). The circuit is governed by a 59 W electric hydraulic pump located in the basement of the building, where all the pipes are arranged together. The pump provides the thermo-vector fluid circulation through the whole system at a maximum flow rate of 210 l h^{-1} and a constant pressure of 2.2 bar. The chosen anti-freeze additive is Propylene Glycol at 25% vol. concentration, which prevents the freezing of the thermo-vector fluid up to a temperature of –20°C. In addition, a heat sink was added to the system in order to dissipate the heat collected during the warm season for simulating the heating activity of a real BTES plant.

As above described, the whole plant was designed with the idea of a high flexibility field scale laboratory. A management system, with a remote control from the Earth Science Department in Torino, was therefore installed to monitor the activity of the plant and to manage it. Several temperature sensors were placed throughout the circuit and within the ground. An energy recorder was moreover installed for the quantification of the energy injected into the ground (produced by the collectors) during the summer and then extracted in the winter period. A website **[54]** was furthermore set up for the dissemination of the project's results.

A total of 20 RTD 4wire Pt100 (measurement range -50 – 180°C, accuracy 5%) were placed every 5 m down-hole in 3 of the 4 BHEs and in the monitoring hole. In addition, 10 temperature sensors of the same type were placed throughout the circuit and on the thermal panels. An ultrasonic flow meter was placed on the pipes for providing flow rate data. Thus, on the strength of temperature T [°C] and flow rate q [m^3 s^{-1}], an energy calculator registers the energy produced by the thermal collectors, by first calculating the instantaneous power P [W] by means of the volumetric heat capacity Cv_w [J m^{-3} K^{-1}]:

$$P = Cv_w \cdot (T_{out} - T_{in}) \cdot q \qquad [2]$$

and then the energy E [Wh] by multiplying it for the working hours. All the sensors were connected to a data logger which continuously collects the data, providing a 0.5 h sample interval.

With the remote control it is possible to visualize and register the temperature sensors' values throughout the circuit and within the ground, selecting and modifying the working modes as well. The operative mode of the system was decided in the light of the several already working plants, where a core volume benefits from the hottest carrier fluid and an annular volume is powered by the same fluid carrying a lower amount of heat. Therefore, the central BHE was used as the warmer core and the externals as a thermal barrier towards the undisturbed ground. During the summer period, the thermo-vector fluid warmed by solar energy is driven down into the central BHE, then out to the hydraulic pump and re-pumped down into the external BHEs afterwards. This is called the "Charge Phase" in which the ground is charged by the thermal energy provided by the Sun and collected by the panels. The system is able to decide whether to circulate the fluid or not, because a temperature difference constraint has been imposed. If the difference between the collectors' and the average ground's temperature is more than 5°C the system works and the ground is charged by solar thermal energy. Conversely, if $\Delta T < 5$°C the circulation is stopped in order to prevent the cooling of the ground. During the winter, the system's circulation is inverted and the "Discharge Phase" occurs. The carrier fluid extracts the heat stored in the ground and brings the energy to the heat sink. The energy calculator placed in the circuit measures the amount of energy injected in the first and extracted in the second phase. The described operative mode has been chosen for the first year of operation (2014).

The plant has been officially launched on April 2 with the charge phase and stopped on October 20. In the first year of operation the discharge phase was not adopted immediately in order to observe the natural cooling of the ground. The decision was led by the fact that the summer 2014 was rather cool with respect to a typical one in these geographical and climatic conditions. Nevertheless, this particular situation will be used for describing the natural discharge and comparing it with the laboratory case study data.

3.3 Numerical model's setup

The numerical simulation of the Grugliasco site was performed with the aim of predicting the extension of the thermal plume through the ground. In this case, all the data collected during the drilling activity and the laboratory analysis, together with information from *Arpa Piemonte* **[51]** and the available literature, were used as input values for the model in order to carry out an as much as possible accurate simulations. The modeling was performed with OpenGeoSys (OGS) code, an open-source initiative for the numerical simulation of thermo-hydro-mechanical/chemical processes. OGS is a flexible numerical framework based on the finite element method, provided to solve multifield problems in porous and fractured media for several geological and hydrological applications. In the numerical environment, a 3D quadrilateral 50 x 50 x 50 m model was developed. A triangular prismatic mesh of about 140,000 elements was set up with Gmesh **[56]** in order to be finer in the center of the model and progressively coarser laterally. The adopted physical properties for the ground are presented in **Tab. 7**.

The numerical model was first calibrated on the experimental data of the first year of operation (2014). The adopted boundary conditions were then used for a long-term simulation aiming at the prediction of the plant's behaviour in the next five years, featuring a 6 month alternation between heat injection and extraction. During the warm season each day should be simulated by an injection at about 40°C for 8 h and at 20°C for the remaining 16 h **[57]**. Nevertheless, this kind of discretization would need excessive computation time. In order to speed up the simulations, a weighted average inlet temperature was therefore chosen: 33°C in the central BHE and 25°C in the externals. During the winter period, an inlet constant temperature of 10°C was adopted. After several comparative tests about time discretization, the whole simulation time was divided in 18,250 steps of 0.1 day each.

4. RESULTS

4.1 Plant's monitoring

A brief report of the registered plant's parameters is reported and commented in the present paper. For a more detailed description please refer to **[58]** and the webpage of the living lab **[54]**. During the first part of the injection period the plant was set to provide the highest possible temperature to the working fluid. The system was therefore set to have a maximum flow rate of 80 - 90 l h^{-1}, which is approximately the 40% of the nominal rate of the pump. On July 10, the working mode was changed by setting the system to optimize the flow rate, with resulting lower fluid temperatures. A lower flow rate allows both the thermo-vector fluid reaching high temperatures and increasing the time of heat release in the ground. In **Fig. 10A** and **Fig. 10B**, data from the sensors placed in the boreholes are reported from April 9 to September 30. Generally, an average increasing temperature trend was observed and heat up rates of 0.4-0.5 °C $month^{-1}$ were registered; data from BHE show however to be strongly influenced during each day by the temperature of the circulating fluid. In the second part of September (from day 140 to the end of the monitored period), several bad weather days influenced the ground temperature, lowering the recorded data in the central borehole (DU) and in one of the externals (A); the monitoring hole (MH) tended to equilibrium. At the end of the whole charging phase, the ground temperature rose approximately to a rather homogeneous value of 16.3-16.4 °C up to 2 m from the central BHE.

A focus on July is reported in **Fig. 11**. The temperature data from sensors in the BHEs and MH are displayed in graph A. The average temperature in BHEs and MH is then compared with those recorded on the collectors (graph B). The inlet and outlet temperature to the BHE field are plotted in comparison with weather data in graph C. Graph D displays the working parameters of the plant (flow rate and instant power) together with the thermal energy progressively produced and injected into the ground. Since July 10, as a consequence of the different operative mode, the flow rate reached values of 200 l h^{-1} (**Fig. 11D**) and immediately some variations of the other parameters were observed. The difference between the inlet temperatures in the DU and in the external BHEs decreased to an average value of 10-15 °C (**Fig. 11C**). The amplitude of the average temperatures in the BHE field increased, with peaks of 21°C (**Fig. 11B**). It is clear in **Fig. 11A** that the amplitude of A and B after this change in flow rate were doubled with respect to the previous condition, whereas the temperature registered in DU remained approximately unchanged. Moreover, it is interesting to note that the MH registered the highest increasing rate in the period since July 20 to 31. This was a late response affected by the high energy production occurred since 8 to 18. Together with June, July was the most productive month among all, with 514 kWh of thermal energy transferred to the ground. It is important to note that this increase in production was registered although the first and the final days of the month saw bad weather conditions with several rainfalls.

In summary, the thermal energy monthly transferred to the ground amounted to 367, 457, 528, 514, 498, 353 and 100 kWh since April to October respectively. On the whole 2,830 kWh (about 10.1 GJ) were injected in seven months. In the light of **Tab. 4**, the total energy which can be potentially produced by the collectors in horizontal position since April to October would be approximately 4.2 MWh (considering 82% efficiency of the *Viotosol* collectors). This divergence should firstly be related to the effective inclination of the collectors on site and secondly to the lower amount of solar radiation received during the 2014 summer.

To estimate the energy transferred to the ground E_T, the total energy produced should be lowered accounting for the losses which occur throughout the circuit, assumed to be approximately 5 - 10%. Therefore, a reference value of E_T = 9.1 GJ can be precautionary accepted. If all the domain influenced by the heat storage is assumed to be affected by a constant temperature increase of 1°C, the ground volume affected by the thermal injection would result in:

$$V = \frac{E_T}{\Delta T * Cv_b} = \frac{9{,}100}{1*2.1} = 4{,}300\ m^3\ .$$

This amount corresponds to a cylinder with a radius of 7 m and a depth of 28 m.

The energy injected, and effectively still present in a volume of cylindrical shape with a 2 m radius (the distance between the monitoring hole and the central BHE), can be estimated by observing the temperature registered in the ground at the end of the injection period. On October 22, the equilibrium temperatures were 16.2°C in the MH, 16.4°C and 16.6°C in the external BHEs, 16.4°C in the central. Therefore, the amount of thermal energy collected E_C is in the range 1.6 - 2.0 GJ, with the two end members corresponding to ΔT = 2°C or 2.5°C respectively.

With the data referring only to the first charge phase, the efficiency of the storage can be estimated to 17 - 22%. A correct estimation of the system's efficiency would be obtained after a complete discharge phase, as the inverted cycle would bring energy to the heat sink. The ratio between injected and extracted energy would output the efficiency of the whole system. It is nevertheless preliminary clear the necessity of an insulation aside the BHEs in order to prevent the dispersion of the heat injected, to improve the storage potential and to facilitate the extraction during the winter season.

4.2 Numerical results

The temperatures registered by the acquisition system were assigned as BC in the model with a discretization equal to the sampling interval (0.5 hours). This input datum is rather heavy from the computational point of view. The comparison between experimental and numerical data is reported in **Fig. 12** (for a simplified visualization one datum per day is reported, averaging the 48 data available for each day). A valid estimation of the real system behavior has been obtained by the numerical simulation. Since July 10, the numerical results show smaller temperature variations (particularly clear in DU) because we changed the inlet temperature by modifying the working mode of the plant. This is also evident in MH, where after a first period with a valid superposition of numerical and experimental data the temperature reached at the end of the simulation is 0.3°C lower than that observed in the field. Obviously, the thermal energy input provided by the plant in the field was the same because a lower temperature is a consequence of a higher flow rate. The monitoring data were therefore not affected by the low inlet temperature. Nevertheless, generally speaking, the values registered in the field are valuably simulated by the code: average errors of 1.54%, 3.36% and 0.64% were achieved for external A, central DU and MH respectively.

The numerical simulation was also adopted to forecast the temperature distribution within the ground in the next years. The weighted average inlet temperature adopted in the charge phase were 24.5°C and 20.3°C in the central and the external BHEs respectively. The outlet temperature in the discharge phase was 10°C in both the borehole types. The simulation outputted a stationary situation during the 5 years, with a very limited ground influence. After the last injection period, the isotherm +2°C shows an extension not bigger than the BHE field and the isotherm +1°C stands at approximately 5 m from the central BHE. The temperature-time prediction's curves in the central BHE and in the MH describe a stationary situation. The ground temperature at the end of each charge-discharge cycle recovers approximately the original temperature with a limited divergence of 0.4 - 0.5°C.

5. DISCUSSION

5.1 General discussion

The temperature monitoring showed that the sensors placed in the BHE grout are very sensitive to the circulation of the thermo-vector fluid. They registered the day/night alternation and a bad weather period is immediately observable in the data recordings. Conversely, the sensors placed in the MH presented a constant temperature increase since April to the end of September. A standalone sensor chain in an independent borehole should be of primary importance in order to correctly monitor the effect of the heating in the ground without the influence of the plant itself.

The different working modes adopted in the injection period revealed different behaviors in the ground. The low flow rate mode, provided until July 10, allowed reaching a high temperature in the circulating fluid, but the amount of heat was almost completely transferred into the ground during the passage in the central BHE. The high flow rate mode, adopted since July 10, provided a lower temperature in the circulating fluid, but the high flow rate guaranteed a more distributed energy transfer among the BHEs.

Periods of about 10 days were compared, two before and two after July 10. As an average, the inlet temperature in the central BHE was clearly bigger during the low flow rate mode, except for isolated peaks influenced by fast-changing conditions. The external inlet temperature was conversely higher after July 10. The energy produced in these four periods was 144, 123, 192 and 130 kWh respectively. The differences seem to be firstly related to the weather conditions and secondarily to the working mode, which did not drastically affect the energy production.

Nevertheless, the high flow rate mode allowed reaching higher temperatures in the external BHEs and thus having a lower thermal gradient between the center of the storage volume and the surrounding environment. In the energy storage applications this is a key factor because the stratification is fundamental for the optimization of the system. In a bigger plant it is crucial to decide whether to have the core dramatically warmer than the annulus or to distribute the heat in a more homogeneous way. In the first case the ground volume could be charged more in the external portions, but at the same time the high thermal gradient would cause high heat transfer within the storage volume and heat losses towards the surrounding (in case of no proper side insulation). In the last case the heat propagation within the storage volume would be minimized, but it would be also difficult to progressively charge the ground.

The numerical simulation was useful to predict the behavior of the ground in the next years of operation of the Grugliasco plant. After the calibration with the monitoring data, a 5 year simulation showed the limited impact of the BHE field in the surrounding environment thanks to the alternating charge/discharge cycle in two different periods of the year. The 10°C inlet temperature during the cold season would cool down the ground in few days, but it would not lower the temperature below the undisturbed ground's value too much.

5.2 Improvement proposals

In the light of the first operative year of the plant,-some possible implementations of the plant can be defined in order to improve its activity.

The direct coupling between the solar panels and the BHE field provided a day/night alternation in the thermal injection. The management system was set up with several conditions which compare the temperature of the carrier fluid in the collectors and the temperature distribution in the BHEs. This prevented the plant to cool down the ground during the night and bad weather days. Nevertheless, a buffer storage could be added to the system in order to limit the alternation and provide the thermal energy at a constant temperature during the warm season. For instance, some other ground thermal energy storage working plants have a short term water tank in order to apply this concept. The collectors warm the fluid up in the tank and this transfers the thermal energy to different portions of the BHE field depending on the temperature of the thermo-vector fluid. As a matter of fact, the energy collected by the Grugliasco plant would increase thanks to a more continuous injection and to lower heat dispersions.

With the calibrated numerical model set up for the simulations, some hypotheses in order to enhance the efficiency of the system can be made. The numerical simulation gives indeed the opportunity to predict what would happen if an insulation was provided around the BHEs. The presence of a ring of insulating material was therefore simulated in order to create a storage volume of cylindrical shape with a radius of 3 m from the central borehole. A thermal conductivity of 0.15 W m^{-1} K^{-1} and a specific capacity of 1,300 J kg^{-1} K^{-1} were assigned to this material, which correspond to the thermal properties of clay. The thickness of this clay barrier is 0.2 m. A similar simulation was therefore carried out and the results are reported in **Fig. 13**. The clay prevents the dispersion of the heat allowing the storage volume to increase the temperature more than in the real case (without the insulation). The temperature reached at 2 m from the source is 18.6°C, with an increase of 2.3°C with respect to the situation without the insulation.

With the numerical data the thermal energy collected by the defined cylindrical volume was therefore calculated. Each element in the cross section was multiplied for the volumetric capacity of the ground in order to obtain the thermal energy collected with that specific temperature increase. If the X-Z slice drawn in **Fig. 13** is assumed to have a thickness of 1 m, the total volume would amount to 180 m^3. The summation of the elements gave as output a stored energy equal to 0.95 GJ which can be correlated to the entire volume (790 m^3) by multiplying it for 790/180 = 4.4. The total E_C in the cylindrical volume surrounded by the clay ring amounts to 4.16 GJ. This value corresponds to the 46% of the total energy produced by the solar collectors (9.1 GJ) and it is clearly higher than the efficiency estimated at field scale without insulation (17%).

It turned out that an insulation ring around the BHEs would guarantee a higher amount of stored energy by doubling that stored without insulation. As a conclusion it can be stated that a thin insulation layer can clearly enhance the storage ability of the ground. The clay has a λ lower than the surrounding ground, but thinking about other materials with even lower thermal properties, it is possible to raise more the collected energy. The role of the insulation would be moreover double, because it would also allow to minimize the environmental impact of the plant.

6. CONCLUSIONS

The study derived from a previous laboratory study encompassing analogical, numerical modeling and geophysical surveys aiming at the thermal characterization of geologic porous media towards their utilization for sensible heat storage (**[1]**, **[2]**). In the light of these laboratory observations, a real field scale system which follows the concept of the ground thermal energy storage was therefore designed. The idea was that of building up a laboratory at field scale in order to assess the ability of the ground to store the heat, to evaluate the influence on the environment of the induced thermal difference. The field scale laboratory provided some fruitful information in the first year of operation. Even though the 2014 warm season did not provide the expected solar energy production, 9.1 GJ of thermal energy were transferred to the unsaturated gravelly-sandy ground since April to the middle of October. In these 7 months, the ground was able to collect approximately the 17% of the total E_T. The main conclusions can be synthesized as follows:

(i) The unsaturated alluvial deposits of the Po Plain revealed to be able to host a BTES plant, showing interesting information about heat storage and transfer concepts already in the first operative year; the Grugliasco plant will be useful to test several methodology for improving the systems' efficiency and their monitoring activity.

(ii) As expected, the direct coupling of the BHEs and the solar panels is not useful for the energy collection. A short term storage could enhance the efficiency of the system by providing thermal energy at a constant temperature.

(iii) Thanks to the numerical simulation, the influence of the Grugliasco plant was predicted. It turned out that the double cycle operative mode (charge + discharge phase) lowers the thermal impact in the surrounding ground. In addition, an insulation ring around the BHE field could enhance the collection efficiency by doubling it.

On the whole, it can be stated that the first charge phase of the Grugliasco plant allowed making numerous observations on several key aspects of the ground thermal energy storage systems. Obviously, these will be taken under consideration when there will be the opportunity to implement the plant or to design and set up a real plant, with its management system and monitoring equipment.

The future research on the Grugliasco plant will focus on the implementation of the BHE field, the evaluation of a possible insulation ring around it and a buffer tank as STS to enhance the energy collection efficiency. Moreover, the implementation of the monitoring equipment will be undertaken, placing temperature sensors down in standalone boreholes and possibly water content sensors.

ACKNOWLEDGEMENTS

The GTES Living Lab in Grugliasco was mainly funded by 2 local project by *Alcotra Innovazione* in 2012 and *P.O.R.-F.E.S.R.* in 2013. Therefore, the authors would like to thank the *Regione Piemonte* for supporting the construction of the plant.

Moreover, the authors would like to express heartfelt thanks to Dr. Eloisa Di Sipio (IGG-CNR of Padua, IT) and Dr. Salvatore Giammanco (INGV of Catania, IT) for the thermal conductivity's measurements with ISOMET 2114 and KD2 Pro devices.

REFERENCES

[1] Giordano N, Comina C, Mandrone G. Laboratory scale analogical and numerical modeling of heat propagation in geologic porous media for thermal characterization towards underground thermal energy storage (UTES) applications. Int J Therm Sci, Unpublished Results. (submitted).
[2] Giordano N., Comina C., Mandrone G. Laboratory scale geophysical measurements aimed at monitoring the thermal affected zone in Underground Thermal Energy Storage (UTES) applications. Geothermics, Unpublished Results. (submitted)
[3] Xu J, Wang RZ, Li Y. A review of available technologies for seasonal thermal energy storage. Sol Energy 2013. doi:10.1016/j.solener.2013.06.006.
[4] Gestore Mercati Energetici - www.mercatoelettrico.org/it accessed 2014 October 14.
[5] N'Tsoukpoe KE, Liu H, Le Pierrès N, Luo L. A review on long-term sorption solar energy storage. Renew Sustain Energy Rev 2009;13:2385–96. doi:10.1016/j.rser.2009.05.008.
[6] Gil A, Medrano M, Martorell I, Lázaro A, Dolado P, Zalba B, et al. State of the art on high temperature thermal energy storage for power generation. Part 1-Concepts, materials and modellization. Renew Sustain Energy Rev 2010;14:31–55. doi:10.1016/j.rser.2009.07.035.
[7] Solar P, Gmbh I. Survey of Thermal Storage for Parabolic Trough Power Plants Period of Performance : Survey of Thermal Storage for Parabolic Trough Power Plants Period of Performance. Contract 2000:61.
[8] International Energy Agency (IEA), SHC Programme, Task 32, Advanced storage concepts for solar and low energy buildings - http://archive.iea-shc.org/index.html accessed 2014 October 5.
[9] International Energy Agency (IEA), SHC Programme, Task 42, Compact thermal energy storage - http://task42.iea-shc.org/ accessed 2014 October 5.
[10] Mugnier D, Goetz V. Energy storage comparison of sorption systems for cooling and refrigeration. Sol Energy 2001;71(1):47–55.
[11] Bales C. Thermal properties of materials for thermo-chemical storage of solar Heat. A Report of IEA SHC Task 32 2005.
[12] Pinel P, Cruickshank C a., Beausoleil-Morrison I, Wills A. A review of available methods for seasonal storage of solar thermal energy in residential applications. Renew Sustain Energy Rev 2011;15:3341–59. doi:10.1016/j.rser.2011.04.013.
[13] Kaygusuz K. The Viability of Thermal Energy Storage. Energy Sources 1999;21:745–55. doi:10.1080/00908319950014489.
[14] Tyagi VV, Buddhi D. PCM thermal storage in buildings – a state of art. Renew Sustain Energy Rev 2007;11(6):1146-66.
[15] Streicher W, Schultz JM, Solè C, Cabeza LF, Bony J, Citherlet S et al. Final report of subtask C "phase change materials". Report C7-IEA SHC Task 32 2008.
[16] Sharma A, Tyagi V V., Chen CR, Buddhi D. Review on thermal energy storage with phase change materials and applications. Renew Sustain Energy Rev 2009;13:318–45. doi:10.1016/j.rser.2007.10.005.
[17] Hadorn JC. Advanced storage concepts for active solar energy-IEA SHC Task 32. In: Eurosun-1st Int Conf Sol Heat Cool Build 2008.
[18] Sharp MK, Loehrke RI. Stratified thermal storage in residential solar energy applications. J Energy 1979;3(2):106-13.
[19] Phillips WF. Effects of stratification on the performance of solar air heating systems. Solar Energy 1981;26:175-80.
[20] Lund PD. Effect on solar thermal behavior in seasonal storage of solar heating systems. Sol Energy 1988;40(3):249-58.
[21] Davidson JH, Adams DA. Fabric stratification manifolds for solar water heating. ASME J Sol Energy Eng 1994;116(3):130-6.

[22] Altuntop N, Arslan M, Ozceyhan V, Kanoglu M. Effect of obstacles on thermal stratification in hot water storage tanks. App Therm Eng 2005;25(14-15):2285-98.
[23] Chung JD, Cho SH, Choon ST, Yoo H. The effect of diffuser configuration on thermal stratification in a rectangular storage tank. Ren Energy 2008;33(10):2236-45.
[24] Dincer I, Rosen MA. Thermal energy storage – Systems and application. 2nd ed. New York: John Wiley & Sons; 2010.
[25] Duffie JA, Beckman WA. Solar engineering of thermal processes. 4th ed. Madison: John Wiley & Sons; 2013.
[26] Fisch MN, Guigas M, Dalenbäck JO. A review of large-scale solar heating systems in Europe. Sol Energy 1998;63(6):355-66.
[27] Oliveti G, Arcuri N, Ruffolo S. First experimental results from a prototype plant for the interseasonal storage of solar energy for the winter heating of buildings. Sol Energy 1998;62:281–90. doi:10.1016/S0038-092X(98)00011-5.
[28] Ucar A, Inalli M. Thermal and economic comparisons of solar heating systems with seasonal storage used in building heating. Renew Energy 2008;33:2532–9. doi:10.1016/j.renene.2008.02.019.
[29] Bauer D, Marx R, Nußbicker-Lux J, Ochs F, Heidemann W, Müller-Steinhagen H. German central solar heating plants with seasonal heat storage. Sol Energy 2010;84:612–23. doi:10.1016/j.solener.2009.05.013.
[30] Dalenbäck JO - http://www.solar-district-heating.eu/ServicesTools/Plantdatabase.aspx accessed 2014 December 10
[31] Schmidt T, Mangold D, Müller-Steinhagen H. Central solar heating plants with seasonal storage in Germany. Sol Energy 2004;76:165–74. doi:10.1016/j.solener.2003.07.025.
[32] Banks D. Thermogeological assessment of open-loop well-doublet schemes: a review and synthesis of analytical approaches. Hydrogeol J 2009;17:1149-55.
[33] Kamal WA. Solar pond literature analysis. Energy Convers Management 1991;32(3):207-15.
[34] Nordell B. Large-scale Thermal Energy Storage 2000:1–10.
[35] Nordell B. Large-scale Utilisation of Renewable Energy Requires Energy Storage Luleå University of Technology Mohamed Grein & Mohamad Kharseh Luleå University of Technology 2007:21–4.
[36] Nordell B. Underground Thermal Energy Storage (UTES). Innostock 2012 2012:1–10. doi:10.2174/97816080528511060101.
[37] Zhao DL, Li Y, Dai YJ, Wang RZ. Optimal study of a solar air heating system with pebble bed energy storage. Energy Convers Management 2011;52:2392–400.
[38] Seibt P, Kabus F. Aquifer thermal energy storage - projects implemented in Germany. ECOSTOCK 2006. In: 10th Int Conf Thermal Energy Storage 2006, Stockton, USA.
[39] Chuard P, Chuard D, Van Gilst J, Hadorn JC, Mercier C. The IEA Task VII, Swiss project in Vaulruz – Design and first experiences. In: SHS 1983, Proc, Part I;195-206.
[40] Schmidt T, Mangold D, Müller-Steinhagen H. Seasonal thermal energy storage in Germany. In: ISES Solar World Congress 2003, June 14-19, Göteborg, Sweden.
[41] DLSC - Drake Landing Solar Community, Borehole thermal energy storage (BTES). http://dlsc.ca accessed 2015 February 10.
[42] Chuard P, Hadorn JC. Central solar heating plants with seasonal storage - heat storage systems: concepts, engineering data and compilation of projects. International Energy Agency 1983, Task VII, Subtask 1c, Switzerland, Sorane, A24398/3, 212 p.
[43] Lundh M, Dalenbäck JO. Swedish solar heated residential area with seasonal storage in rock: Initial evaluation. Renew Energy 2008;33:703–11. doi:10.1016/j.renene.2007.03.024.
[44] Project description of the Emmaboda BTES plant, Sweden - www.icax.co.uk accessed 2014 October 4.
[45] Currency conversions - http://fxtop.com accessed 2014 November 25.
[46] Global irradiation data in Europe - http://solargis.info accessed 2014 October 13.
[47] Project description of the Crailsheim BTES plant, Germany - www.solites.de accessed 2014 October 4.
[48] Henrik B. Borehole thermal energy storage in combination with district heating. Proc European Geothermal Congress 2013, June 3-7, Pisa, Italy, SG5-01.
[49] PVGIS - http://re.jrc.ec.europa.eu/pvgis/apps4/pvest.php?lang=en&map=Europe accessed 2014 November 5
[50] Weather Station UNITO Physics Department - www.meteo.dfg.unito.it accessed 2015 February 10
[51] GeoPortale Arpa Piemonte – http://webgis.arpa.piemonte.it/geoportale/ accessed 2014 November 10
[52] Polino R. Note illustrative della Carta Geologica d'Italia alla scala 1:50.000, Foglio 155 Torino Ovest. Progetto CARG ISPRA 2010, Centro Regionale per le Ricerche Territoriali e Geologiche, Arpa Piemonte
[53] Carrier WD. Goodbye, Hazen; Hello, Kozeny-Carman. J Geotech Geoenvironmental Eng 2003;129:1054–6. doi:10.1061/(ASCE)1090-0241(2003)129:11(1054).

PRE-PRINT VERSION OF THE MANUSCRIPT PUBLISHED ON RENEWABLE ENERGY BY ELSEVIER
Please cite this Manuscript as Giordano N., Comina C., Mandrone G., Cagni A. (2016) – Borehole thermal energy storage (BTES). First results from the injection phase of a living lab built up in unsaturated alluvial deposits (Torino, IT). Renewable Energy, 86: 993-1008.

[54] GTES Grugliasco Living Lab – www.gtes.unito.it accessed 2015 February 10.
[55] Kolditz O, Bauer S, Bilke L, Böttcher N, Delfs JO, Fischer T, et al. OpenGeoSys: An open-source initiative for numerical simulation of thermo-hydro-mechanical/chemical (THM/C) processes in porous media. Environ Earth Sci 2012;67:589–99. doi:10.1007/s12665-012-1546-x.
[56] Geuzaine C, Remacle JF. Gmsh: a three-dimensional finite element mesh generator with built-in pre- and post-processing facilities. Int J Num Method Eng 2009;79(11):1309-31.
[57] Diersch HJG, Bauer D, Heidemann W, Rühaak W, Schätzl P. Finite element modeling of borehole heat exchanger systems. Part 2. Numerical simulation. Computers & Geosciences 2011; 37:1136-47.
[58] Giordano N. Ground Thermal Energy Storage: analogical and numerical modeling coupled with geophysical monitoring from laboratory to field scale. PhD thesis 2015, 236 p. doi:10.13140/2.1.3671.5843.

Captions

Fig. 1 - Volume needed to store 10 GJ with different storage mechanisms with a ΔT of 70°C (modified from **[17]**).

Fig. 2 - Vertical BHEs linked together to exploit the ground as a storage volume in a closed-loop system. The core presents higher temperatures than those in the annular zone in order to minimize the heat losses towards the surrounding undisturbed ground.

Fig. 3 - Horizontal closed-loop system constructed in Vaulruz, CH (modified from **[39]**).

Fig. 4 – Comparison between the 2014 daily temperatures and monthly rainfalls and the average values for the past years (2005-2013).

Fig. 5 - Geographical and geological test site location.

Fig. 6 - Stratigraphic section of the examined area (data from **[51]**).

Fig. 7 - Grain size distribution of the 3 collected samples.

Fig. 8 – Pictures of the living lab. Drilling activity in front of the Topography department (A-B); temperature sensors placed throughout the circuit (C); ultrasonic flow meter (D); hydraulic circuit of the plant (E); underground section of the remote control system (F).

Fig. 9 - Satellite image **[51]** of the test site area. The arrangement of the BHEs and the monitoring hole are reported with the indication of the boreholes equipped with temperature sensors. The green roof is that of the Topography building where the solar collectors are placed.

Fig. 10 – Whole registration period (April 8 – October 20). DU, A, B = central and external BHEs. MH = monitoring hole. Uppermost graph: temperature data from the central borehole (green) with the regression curve referred to the daily minimum (orange). Lowermost graph: temperature data from the A borehole (blue) and the MH (violet) with the regression curves, referred to the daily minimum (red) for A.

Fig. 11 July data. DU, A, B = central and external BHEs. MH = monitoring hole. IN, OUT = inlet and outlet temperature to the BHE field. SR = daily max solar radiation. Description about each graph are reported in the text.

Fig. 12 – Comparison between the field data monitored by the system (“exp”) and the numerical results of the simulation (“num”) in external BHE (A), central BHE (DU) and monitoring hole (MH). The data are daily averages.

Fig. 13 – Results of the simulation with the clay ring as insulation technique. The X-Y plan view (left) and the X-Z cross section (right) are reported.

LIST OF SYMBOLS

GENERIC SYMBOLS

Symbol	***Description***	***Unit of measure***
Cs_b	bulk specific heat capacity	[J kg^{-1} K^{-1}]
Cv_w	water volumetric heat capacity	[J m^{-3} K^{-1}]
d_0	mean diameter of spherical grains	[mm]
E	energy	[J] or [Wh]
E_C	energy collected by the ground	[J] or [Wh]
E_T	energy transferred to the ground	[J] or [Wh]
P	instantaneous power	[W]
q	flow rate	[l s^{-1}] or [m^3 s^{-1}]

q'	energy input	[W m^{-1}]
SR	solar radiation	[W m^{-2}]
t	time	[s]
T	temperature	[°C] or [°K]
V	volume domain	[m^3]

GREEK SYMBOLS

Symbol	***Description***	***Unit of measure***
γ_b	bulk density	[kg m^{-3}]
ΔT	temperature difference	[°C] or [°K]
λ	thermal conductivity	[W m^{-1} K^{-1}]

ACRONYMS

A, B	Single U piped BHEs
AT	Austria
BHEs	Borehole Heat Exchangers
BTES	Borehole Thermal Energy Storage
CH	Switzerland
DHW	Domestic Hot Water
DU	Double U piped BHE
ENEA	Italian agency for new technologies, energy and sustainable economic development
FTP	File Transfer Protocol
GCHPs	Ground Source Heat Pumps
H&C	Heating and Cooling
IEA	International Energy Agency
ISO	Isomet 2114 device
IT	Italy
K2D	K2D Pro device
LT	Long Term
MH	Monitoring hole
NL	The Netherlands
OGS	OpenGeoSys
PCMs	Phase Change Materials
RES	Renewable Energy Sources
SE	Sweden
SHC	Solar Heating Cooling programme
ST	Short Term
STES	Seasonal Thermal Energy Storage
TCMs	Thermo-Chemical Materials
TES	Thermal Energy Storage

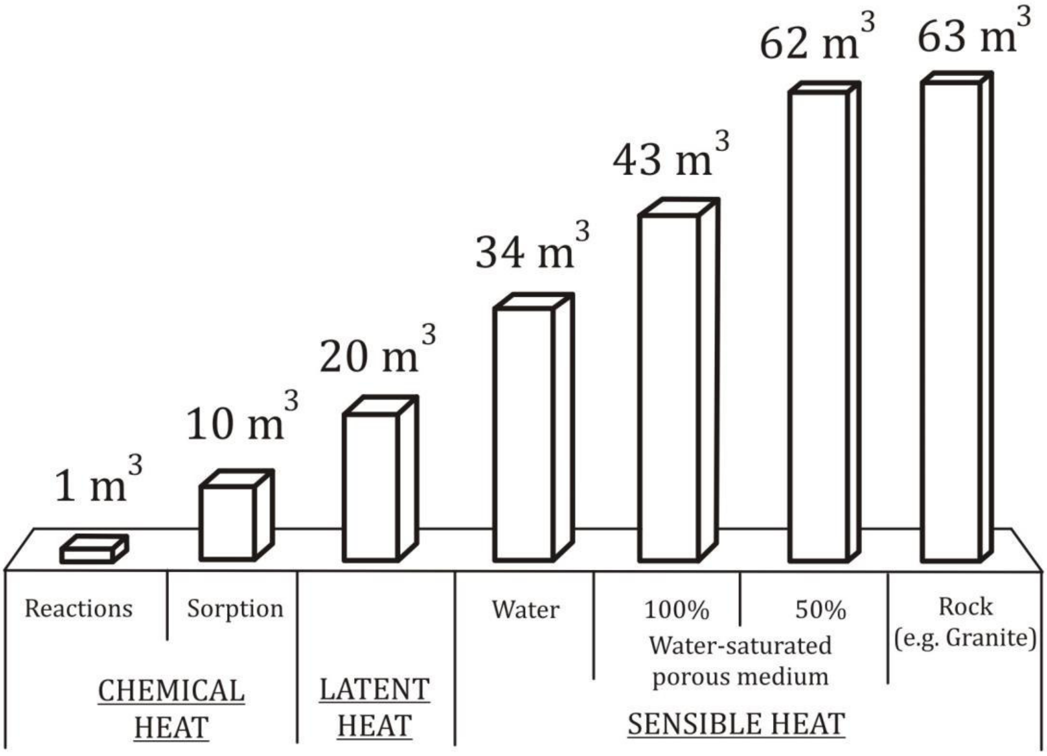

Fig. 1 - Volume needed to store 10 GJ with different storage mechanisms with a ΔT of 70°C (modified from **[17]**).

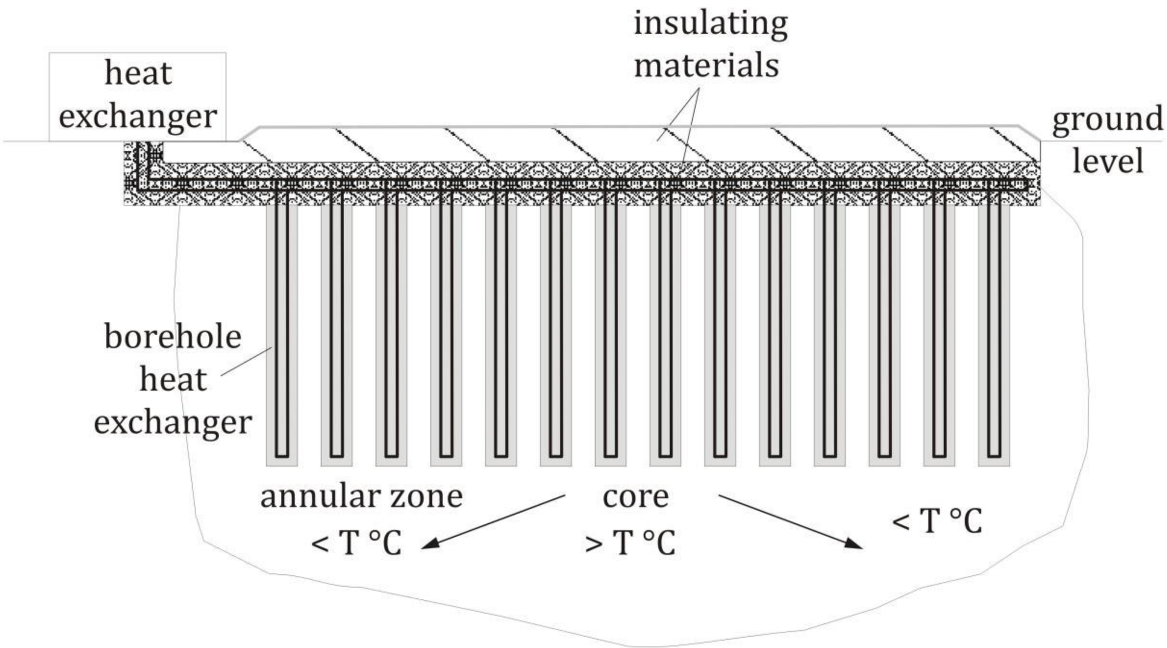

Fig. 2 - Vertical BHEs linked together to exploit the ground as a storage volume in a closed-loop system. The core presents higher temperatures than those in the annular zone in order to minimize the heat losses towards the surrounding undisturbed ground.

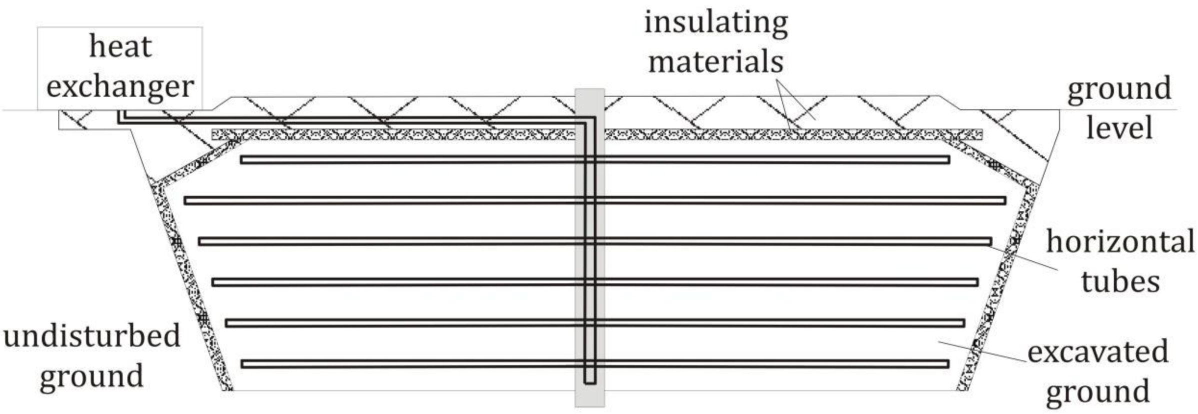

Fig. 3 - Horizontal closed-loop system constructed in Vaulruz, CH (modified from **[39]**).

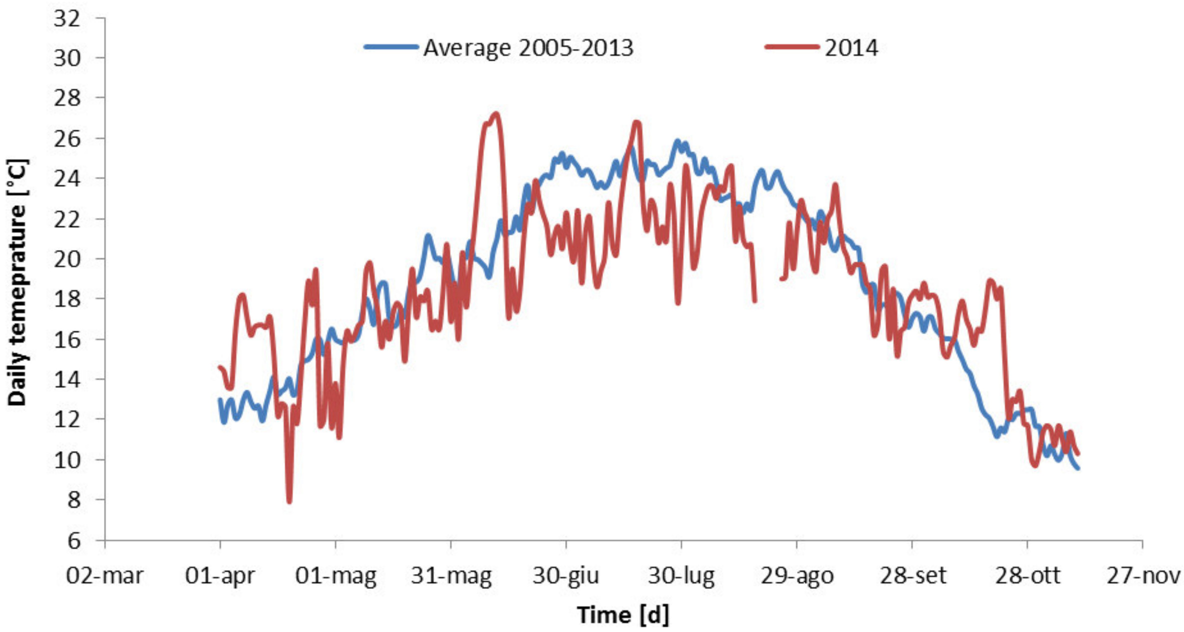

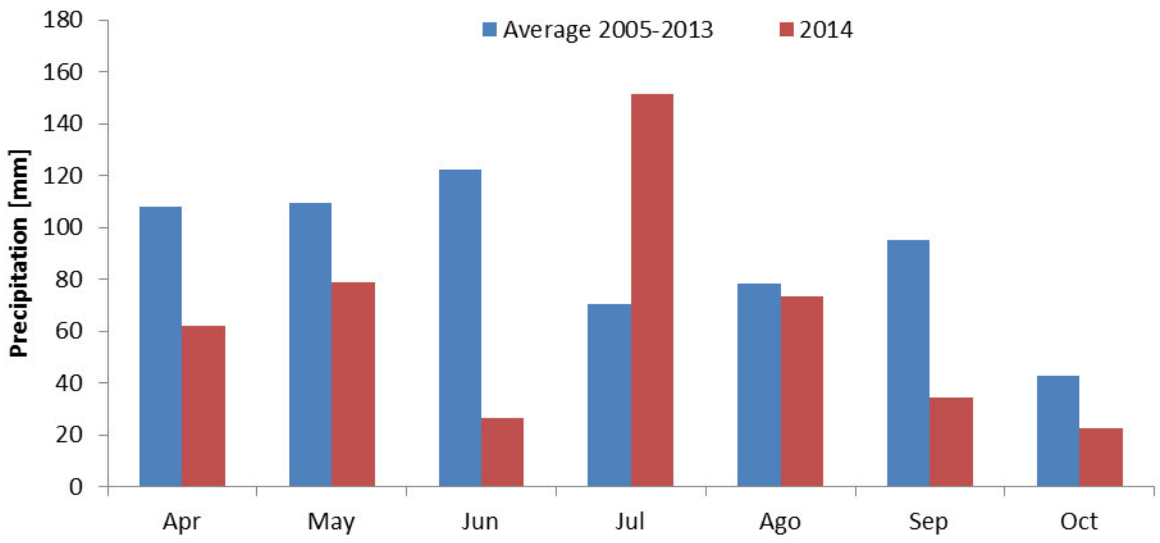

Fig. 4 – Comparison between the 2014 daily temperatures and monthly rainfalls and the average values for the past years (2005-2013).

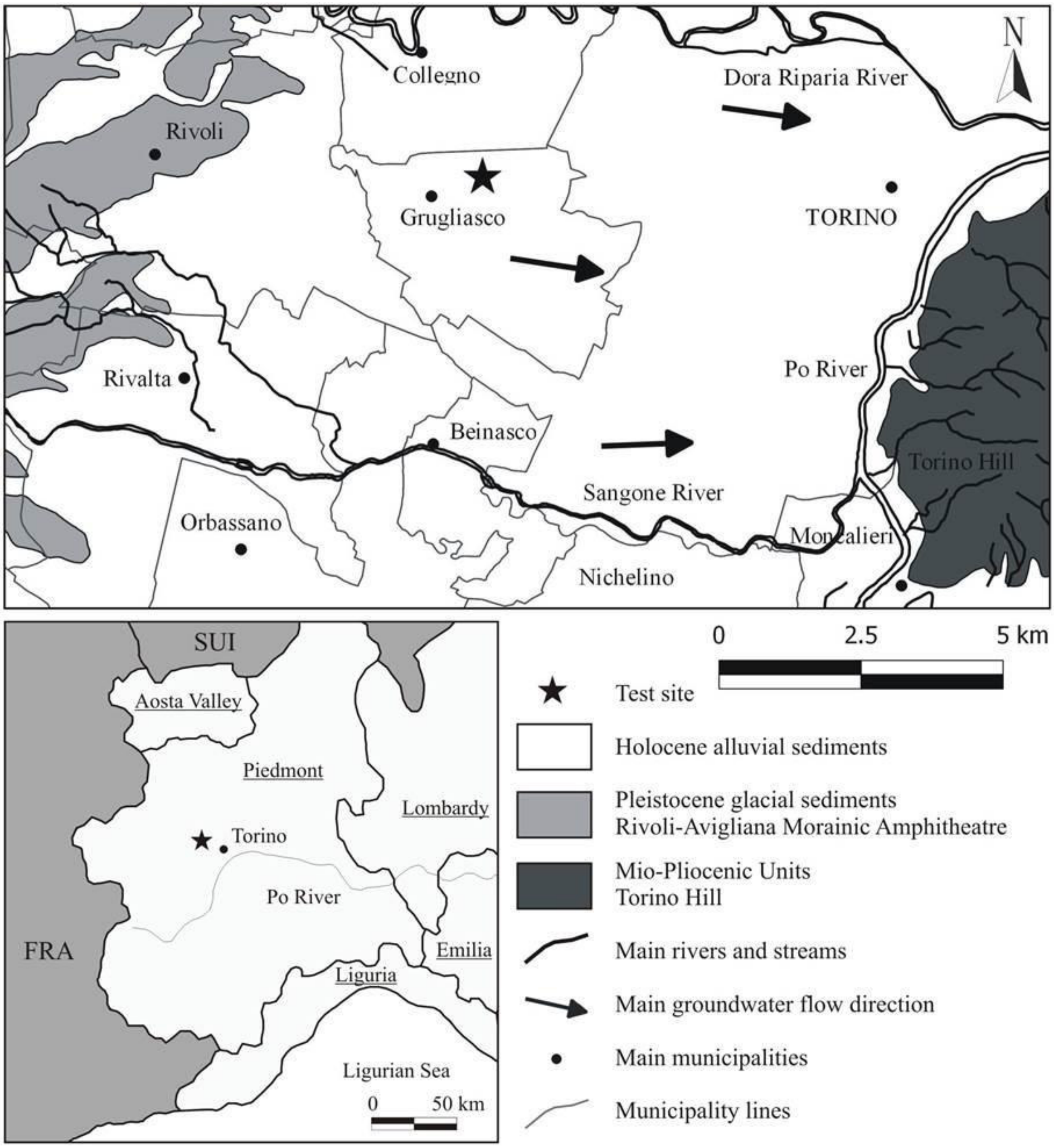

Fig. 5 - Geographical and geological test site location.

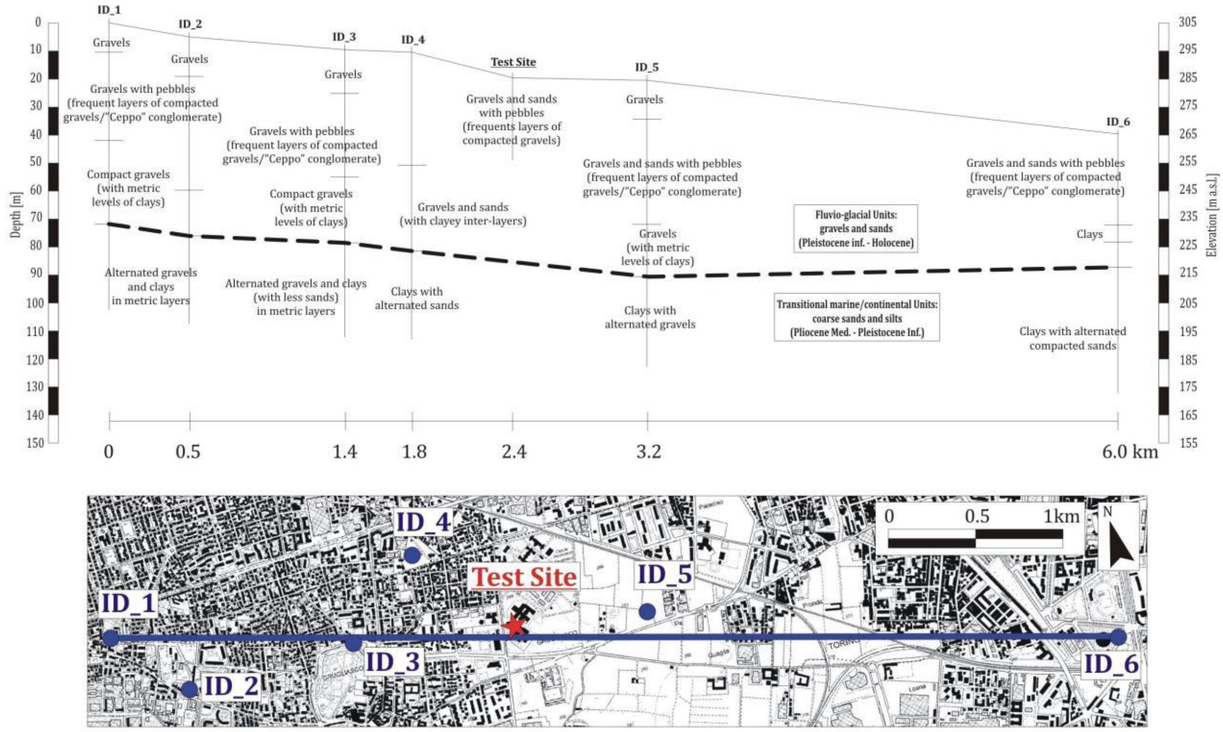

Fig. 6 - Stratigraphic section of the examined area (data from **[51]**).

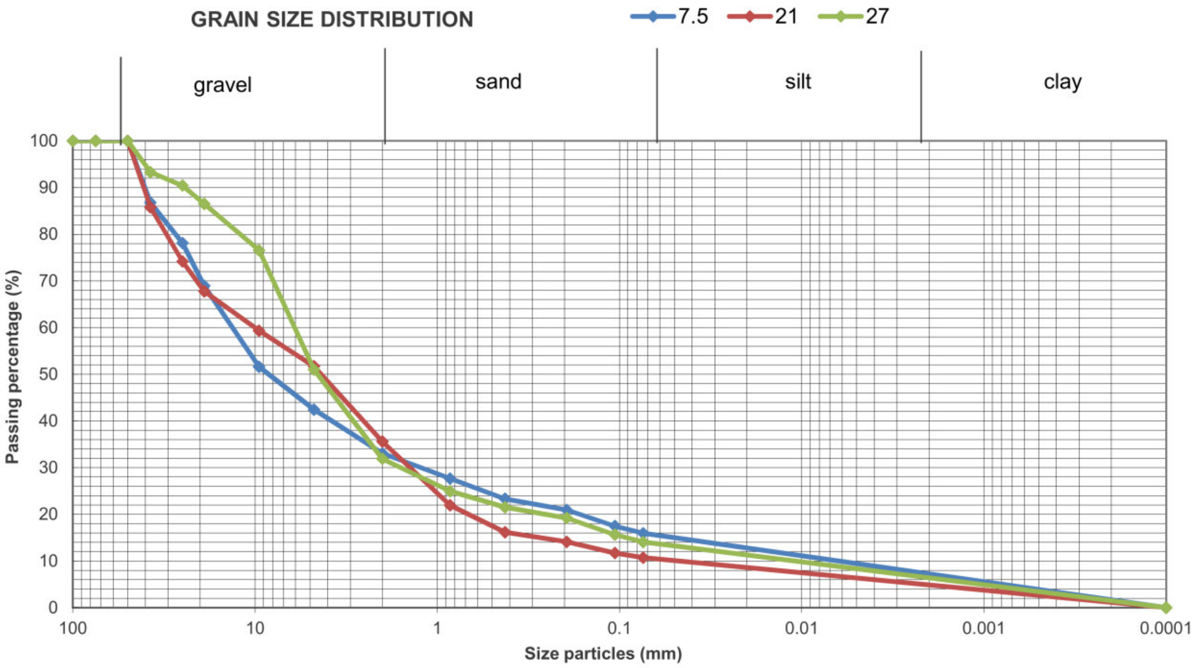

Fig. 7 - Grain size distribution of the 3 collected samples.

Fig. 8 – Pictures of the living lab. Drilling activity in front of the Topography department (A-B); temperature sensors placed throughout the circuit (C); ultrasonic flow meter (D); hydraulic circuit of the plant (E); underground section of the remote control system (F).

Fig. 9 - Satellite image **[51]** of the test site area. The arrangement of the BHEs and the monitoring hole are reported with the indication of the boreholes equipped with temperature sensors. The green roof is that of the Topography building where the solar collectors are placed.

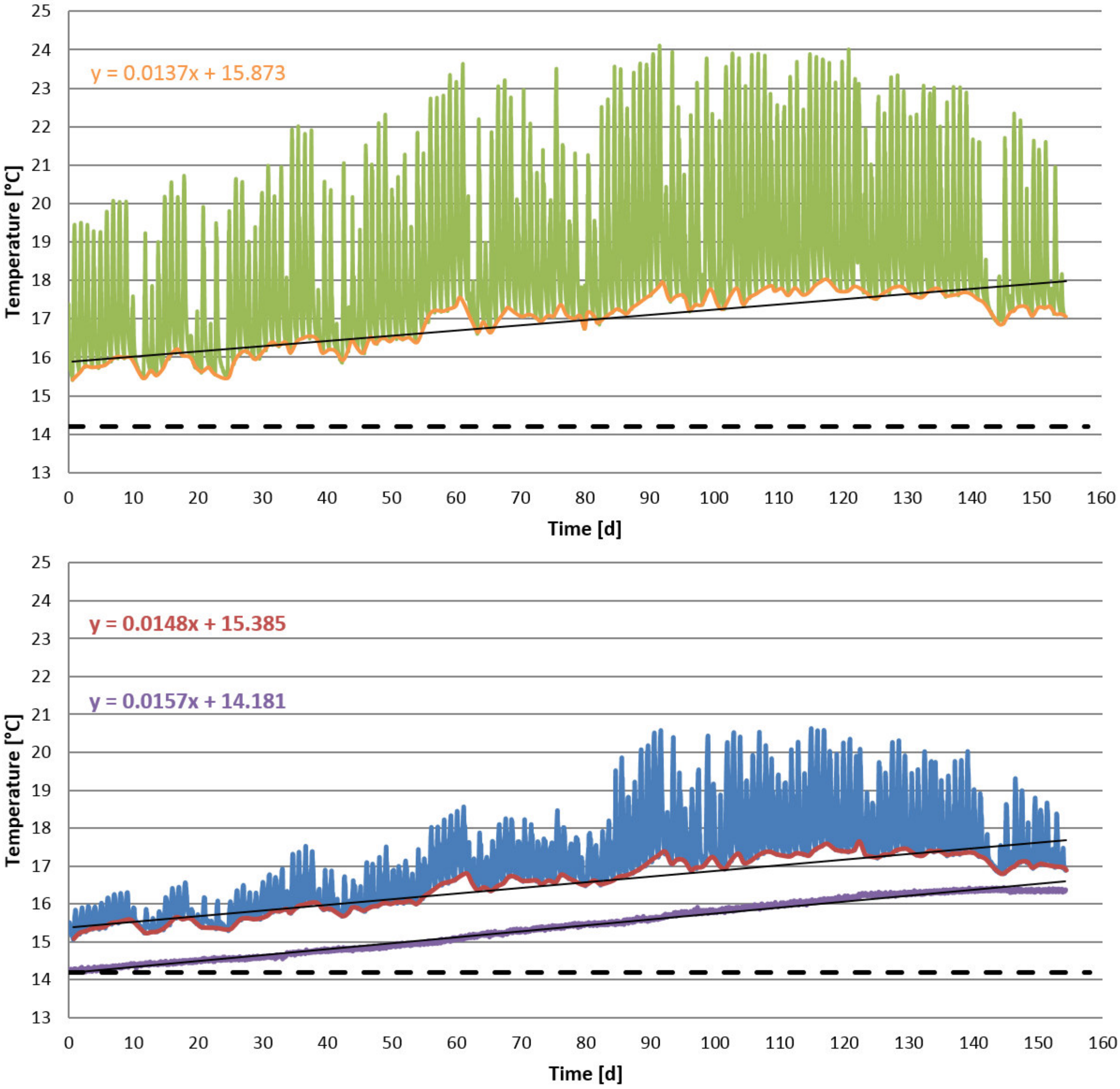

Fig. 10 – Whole registration period (April 8 – October 20). DU, A, B = central and external BHEs. MH = monitoring hole. Uppermost graph: temperature data from the central borehole (green) with the regression curve referred to the daily minimum (orange). Lowermost graph: temperature data from the A borehole (blue) and the MH (violet) with the regression curves, referred to the daily minimum (red) for A.

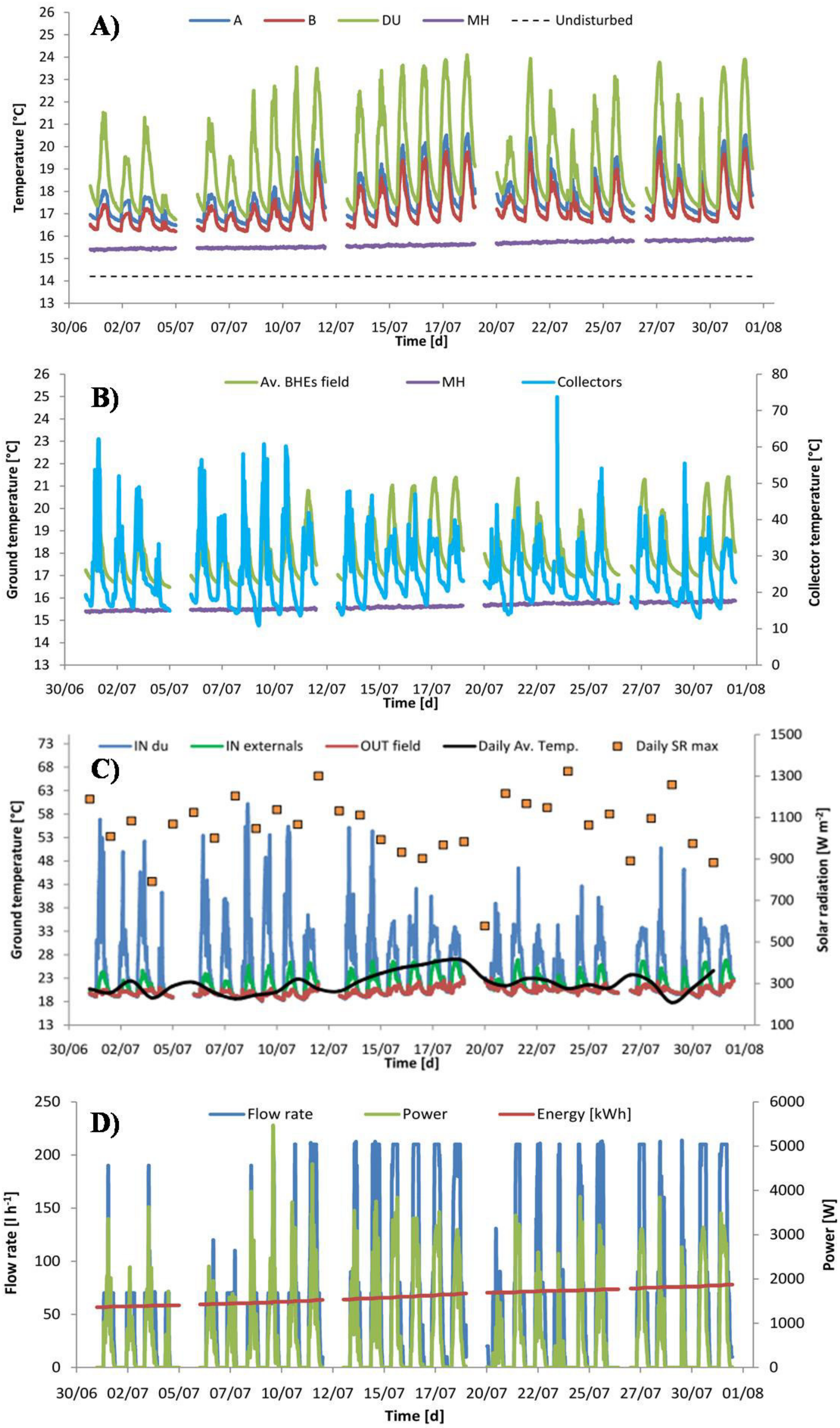

Fig. 11 July data. DU, A, B = central and external BHEs. MH = monitoring hole. IN, OUT = inlet and outlet temperature to the BHE field. SR = daily max solar radiation. Description about each graph are reported in the text.

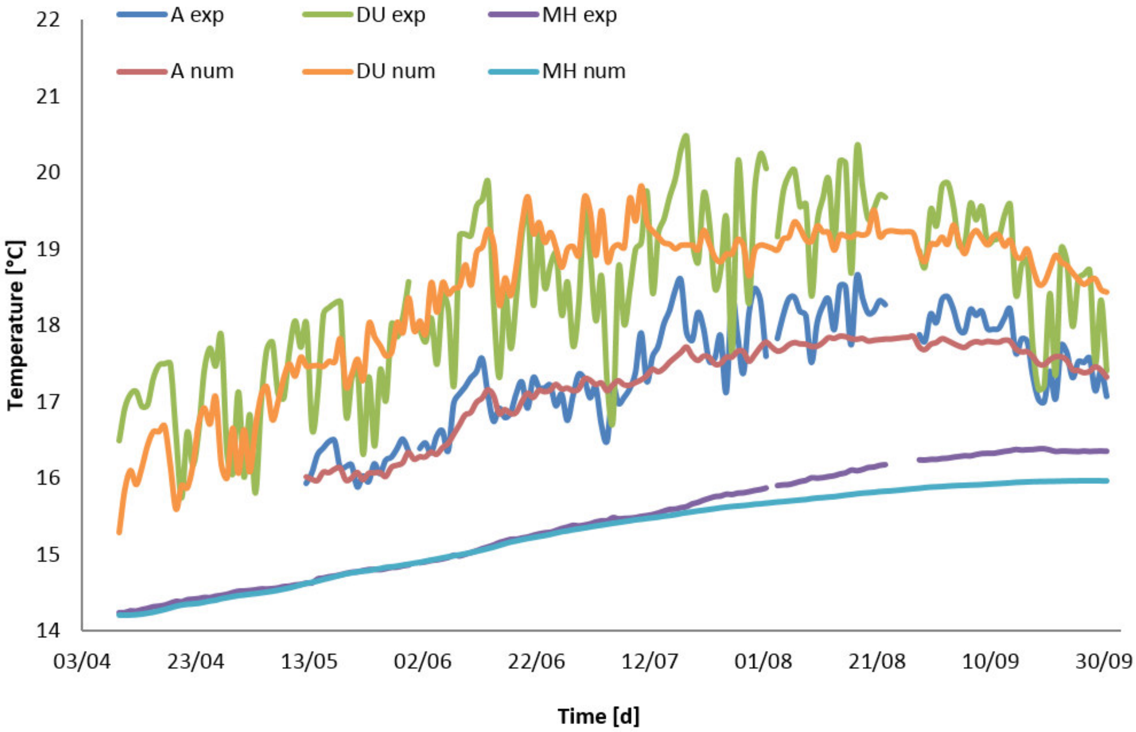

Fig. 12 – Comparison between the field data monitored by the system ("exp") and the numerical results of the simulation ("num") in external BHE (A), central BHE (DU) and monitoring hole (MH). The data are daily averages.

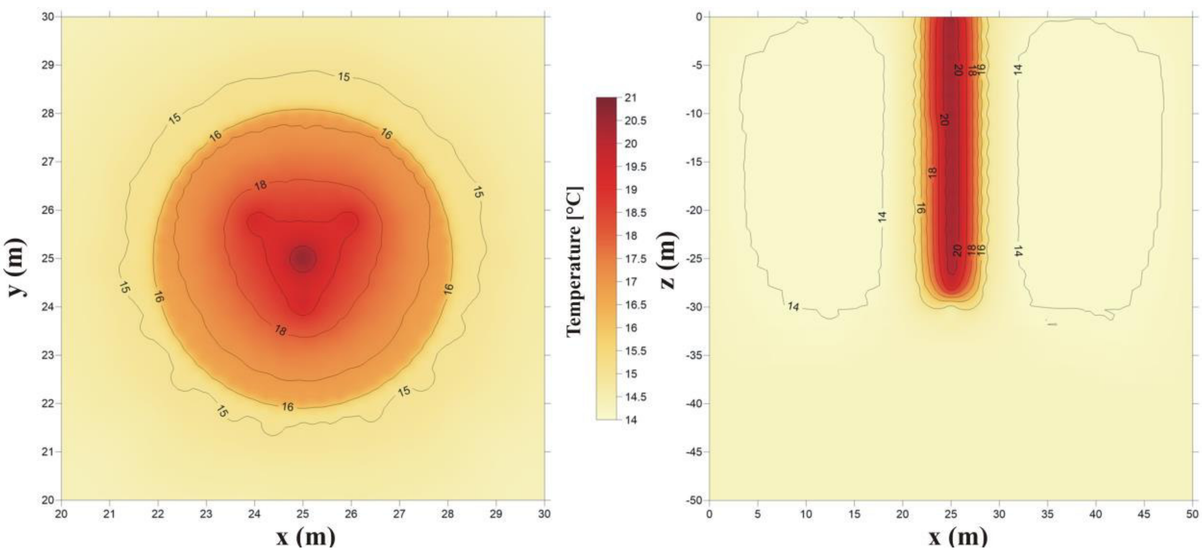

Fig. 13 – Results of the simulation with the clay ring as insulation technique. The X-Y plan view (left) and the X-Z cross section (right) are reported

Tab. 1 – Borehole thermal energy storage (BTES) projects constructed in Sweden (**[42]**, **[43]**).

Site	-	Kungsbacka, SE	Store Skuggan, SE	Södertuna, SE	Luleå, SE	Danderyd, SE	Emmaboda, SE[(1)]
Start-up	year	1980	1982	1982	1983	2002	2010
Housing area	-	1 school	-	525 houses	1 university building	50 houses	Factory building
Global irradiation (Hz)	kWh m^{-2}	940	-	370	-	-	-
Heating degree-days (ref. 20°C)	°C	-	5,000	-	6,250	-	-
Heated living area	m^2	-	-	-	-	6,000	-
Total heat demand	MWh y^{-1}	1,100	500	6,390	-	550	-
Solar collector area	m^2	1,500	2,200	30,000	(no solar energy but waste heat)	2,400	(no solar energy but waste heat)
Heat storage volume	m^3	85,000 (BTES)	180,000 + 1,000 (BTES + hot-water STS)	105,000	120,000	60,000	200,000
Geologic material	-	Clay	Gneiss and granite	Granite	Gneiss	Granite	Gneiss
Extracted heat from BTES	MWh y^{-1}	710	430	4,160	1,100	385	3,000
Solar fraction	%	65	85	65	-	70	-
Cost of the system (solar + storage)	M€ [(2)]	0.17	1.03	2.7	0.85	0.54	-

[(1)] Data from **[44]**
[(2)] Currency conversion functions from **[45]**

Tab. 2 – Borehole thermal energy storage (BTES) projects until 1990 (**[26]**, **[42]**).

Site	-	Innsbruck, AT	Groeningen, NL	Vaulruz, CH	Ispra, IT	Treviglio, IT
Start-up	year	1980	1982	1982	1982	1985
Housing area	-	1 airport	96 houses	1 maintenance centre	1 JRC building	residential area
Global irradiation (Hz)	kWh m^{-2}	1,090	910	1,180	1,160	1,200 (1)
Heating degree-days (ref. 18°C)	°C	3,235 (2)	3,000	3,886	2,500 (3)	
Heated living area	m^2	-	-	-	-	
Total heat demand	MWh y^{-1}	1,220	1,140	340	80	
Solar collector area	m^2	400	2,400	510		2,727
Heat storage volume	m^3	60,000 + 40 (BTES + hot-water STS tank)	23,000 + 100 (BTES + hot-water STS tank)	3,500 (BTES with horizontal pipes)	2,250 + 80 (BTES + hot-water STS tank)	43,000
Geologic material	-	Gravel	Saturated sand with clay and peat layers	Sandy gravel with clay	Clay	
Heat delivery of the solar system	MWh y^{-1}	640	760	220	64	
Solar fraction	%	52	67	65	80	70
Cost of the system (solar + storage)	M€(4)	-	0.71	0.31	-	

(1) Deduced from **[46]**
(2) Reference value 12 °C
(3) Reference value 15 °C
(4) Currency conversion functions from **[45]**

Tab. 3 – Borehole thermal energy storage (BTES) projects from 1990 up to now.

Site		**Neckarsulm, DE Phase I (Phase II)** [(1)]	**Attenckirchen, DE** [(1)]	**Crailsheim, DE Phase I** [(2)]	**Okotoks, CA** [(3)]	**Braedstrup, DK** [(4)]
Start-up	year	1996	1999	2006	2006	2012
Housing area	-	6 multi-family houses, commercial centre, school	30 apartments in single-family houses	260 apartments, 1 school and 1 sports hall	52 apartments in single-family houses	District heating plant, 1,500 consumers
Global irradiation (Hz)	kWh m^{-2}	1,100 [(5)]	1,100 [(5)]	1,100 [(5)]	1,510	1,100[(5)]
Heating degree-days (ref. 18°C)	°C	-	-	-	4,910	-
Heated living area	m^2	20,000	6,200	40,000	6,800	-
Total heat demand	MWh y^{-1}	1,663	487	4,100	790	3,600
Solar collector area	m^2	2,700 (5,000)	800	7,300	2,300	18,600
Heat storage volume	m^3	20,000 (63,400) (BTES)	9,350 + 500 (BTES + hot water STS tank)	37,500 + 580 (BTES + hot-water STS tank)	35,600 + 240 (BTES + hot water STS tank)	19,000 + 7,500 (BTES + 2 hot water tanks)
Geologic material	-	-	-	Limestones	-	Clay till and sands and gravels
Heat delivery of the solar system	MWh y^{-1}	832	415	2,050	682	7,000
Solar fraction	%	50	55	50	86	20
Cost of the system (solar + storage)	M€ [(6)]	1.5	0.26	4.5	2.3	4.3

[(1)] Data from **[30]** [(2)] Data from **[47]** [(3)] Data from 2011 annual report **[41]**
[(4)] Data from **[48]** [(5)] Deduced from **[46]** [(6)] Currency conversion functions from **[45]**

Tab. 4 – Solar energy data of the Grugliasco area with the indication of the optimal inclination of a collector aiming at the maximum production (**[49]**).

Month	Global irradiation (Hz) [Wh m^{-2} day^{-1}]	Optimal inclination [°]	Average air temperature [°C]	Heating degree-days [°C]
Jan	1,520	66	3.9	410
Feb	2,070	57	5.6	328
Mar	3,520	46	9.1	221
Apr	4,390	30	12.0	112
May	5,090	17	17.0	12
Jun	6,040	12	20.9	0
Jul	6,310	15	22.9	0
Aug	5,480	26	22.5	1
Sep	4,060	41	18.5	42
Oct	2,590	53	14.3	184
Nov	1,590	63	8.4	352
Dec	1,220	67	4.8	430
Year	3,670	37	13.3	2,092

Tab. 5 – Thermal conductivity measurements on the ground's samples.

Samples' depth [m]	Thermal Conductivity [W m^{-1} K^{-1}]		Device
	dry	water saturated	
7.5	0.47±0.02	2.55±0.04	ISOMET 2114
21	0.55±0.02	2.52±0.05	ISOMET 2114
27	0.45±0.03	2.31±0.07	KD2 Pro

Tab. 6 – Thermal conductivity measurements on the grout's samples.

Samples	Thermal Conductivity [W m^{-1} K^{-1}]		Device
	dry	water saturated	
1	0.77±0.03	0.93±0.01	ISOMET 2114
2	0.69±0.09	0.84±0.04	ISOMET 2114
3	0.67±0.01	0.83±0.01	ISOMET 2114
4	0.64±0.01	-	ISOMET 2114
5	0.73±0.01	0.62±0.12	ISOMET 2114
6	0.40±0.01	0.78±0.00	ISOMET 2114
7	0.31±0.08	-	KD2 Pro
8	0.27±0.05	-	KD2 Pro

Tab. 7 – Numerical model properties adopted in the OGS simulation.

Undisturbed *T* [°C]	14.2
Porosity	0.3

Water content [%]	50
Water density [kg m^{-3}]	1,000
Water specific heat capacity [J kg^{-1} K^{-1}]	4,190
Water thermal conductivity[W m^{-1} K^{-1}]	0.6
Air density [kg m^{-3}]	1.2
Air specific heat capacity [J kg^{-1} K^{-1}]	1,010
Air thermal conductivity[W m^{-1} K^{-1}]	0.024
Solid density [kg m^{-3}]	2,700
Solid specific heat capacity [J kg^{-1} K^{-1}]	800
Solid thermal conductivity[W m^{-1} K^{-1}]	3.0
Grout thermal conductivity [W m^{-1} K^{-1}]	0.45